The Journal of Chemical Physics

RESEARCH ARTICLE | JUNE 08 2023

Investigating the role of carbon doping on the structural and energetic properties of small aluminum clusters using quantum Monte Carlo FREE

B. G. A. Brito ; G.-Q. Hai ; L. Cândido

J. Chem. Phys. 158, 224305 (2023)
https://doi.org/10.1063/5.0156315

The Journal of Chemical Physics ARTICLE scitation.org/journal/jcp

Investigating the role of carbon doping on the structural and energetic properties of small aluminum clusters using quantum Monte Carlo

Cite as: J. Chem. Phys. 158, 224305 (2023); doi: 10.1063/5.0156315
Submitted: 28 April 2023 • Accepted: 23 May 2023 •
Published Online: 8 June 2023

B. G. A. Brito,[1] G.-Q. Hai,[2] and L. Cândido[3,a)]

AFFILIATIONS

[1] Departamento de Física, Instituto de Ciência Exatas e Naturais e Educação, Universidade Federal do Triângulo Mineiro, 38064-200 Uberaba, MG, Brazil
[2] Instituto de Física de São Carlos, Universidade de São Paulo, 13560-970 São Carlos, SP, Brazil
[3] Instituto de Física, Universidade Federal de Goiás, 74001-970 Goiânia, GO, Brazil

[a)] **Author to whom correspondence should be addressed:** ladir@ufg.br

ABSTRACT

In this study, we investigate the energetics of small aluminum clusters doped with a carbon atom using several computational methods, including diffusion quantum Monte Carlo, Hartree–Fock (HF), and density functional theory. We calculate the lowest energy structure, total ground-state energy, electron population distribution, binding energy, and dissociation energy as a function of the cluster size of the carbon-doped aluminum clusters compared with the undoped ones. The obtained results show that carbon doping enhances the stability of the clusters mainly due to the electrostatic and exchange interactions from the HF contribution gain. The calculations also indicate that the dissociation energy required to remove the doped carbon atom is much larger than that required to remove an aluminum atom from the doped clusters. In general, our results are consistent with available theoretical and experimental data.

I. INTRODUCTION

In recent years, considerable efforts have been devoted to searching for atomic clusters that could be candidates for building cluster-based materials that could give rise to new materials with unique properties. These clusters must be stable enough to retain their shape and properties when assembled into cluster-based materials.[1] It is known that the stability of clusters is related to the electronic and atomic structures and that there are some special clusters called "magic clusters" that are suitable for such requirements.[2] Among the various metallic clusters studied, aluminum clusters and doped aluminum clusters have received much attention because of the role of the electronic properties of aluminum in semiconductor structures. The jellium model explains the high stability of some pure aluminum clusters such as Al_7^+ and Al_{13}^-, which contain 20 and 40 valence electrons, respectively.[3–5] Although these clusters are very stable, they cannot be used to build new materials because they are charged. To overcome this limitation, researchers have explored doping aluminum clusters with different atoms, resulting in the stabilization of certain clusters such as Al_{12} and Al_{13}, which can be used to create cluster-based materials with distinct properties. These materials have potential for various applications due to their unique properties.

Among several types of atoms that can be used to dope the aluminum clusters, carbon has received considerable experimental[6–8] and theoretical[6,9–11] attention. Carbon is a tetravalent atom found in two solid forms in nature: diamond and graphite, where the carbon forms covalent bonds and presents fourfold and threefold coordination, respectively. However, in carbon–aluminum clusters, the carbon exhibits different bonding behaviors, depending on the size and charge state of the cluster. In such clusters, the carbon can bond more than four aluminum atoms and have a coordination number different from the usual three- or fourfold coordination number, as has been observed for $Al_{12}C$.[12] The carbon–aluminum

clusters have interesting structures and properties depending on the size of the clusters. The Al_3C presents halogen characteristics with a smaller electron affinity than the iodine atom.[9] Among the small carbon–aluminum clusters, the Al_4C and $Al_{12}C$ have attracted special attention since they are closed-shell systems with considerable structural stability. They are sometimes called magic clusters.[8,11]

In this paper, we have studied the structural and electronic properties of small neutral carbon–aluminum clusters $Al_{n-1}C$ $(n = 2, 3, \ldots, 13)$ to better understand the influence of carbon on the physical and chemical properties of this system. To this end, we use the fixed-node diffusion quantum Monte Carlo (FN-DMC) method to obtain a very accurate estimate of the ground-state energy as a function of the cluster size n. We have determined the binding energy and dissociation energy of these clusters. In order to make the electronic correlation effects explicit, we have also performed the calculations within the Hartree–Fock (HF) theory in the complete basis set limit. Together with the ground-state energies obtained from the FN-DMC calculations, we extract the correlation energies.

II. THEORETICAL APPROACH AND COMPUTATIONAL DETAILS

We use density functional theory (DFT) and quantum Monte Carlo (QMC) simulations to study the electronic properties of the carbon-doped small aluminum clusters. The calculations were performed in two parts. First, the atomic structure of the cluster is studied within the density functional theory (DFT)[13,14] using the exchange–correlation potential of Becke[15] and the nonlocal correlation functional of Lee, Yang, and Parr (LYP)[16] using the Gaussian program[17] with 6-311++G(2d,2p) basis set.[18] The Dirac–Fock average relativistic effective potential (AREP) is used to represent the core electrons.[19,20] Subsequently, the quantum Monte Carlo (QMC) methods are used to study the electronic structure calculations with the CASINO code.[21] We performed the QMC calculations in two steps, first using the variational Monte Carlo (VMC) method to obtain an optimized Slater–Jastrow type trial wave function defined as follows:

$$\psi_T(R) = D_\uparrow(\phi_i) D_\downarrow(\phi_i) e^U, \tag{1}$$

where R is the electronic configuration, $D_\uparrow$ and $D_\downarrow$ are the determinants of the up- and down-spin orbitals, respectively, and ϕ' are the single-particle orbitals extracted from a DFT calculation using the Gaussian03 code.[17] The Jastrow factor U in Eq. (1) is a sum of homogeneous, isotropic electron–electron terms $u(r_{ij}, \alpha)$, isotropic electron–core terms $\chi(r_{iI}, \beta)$ centered on the core, and isotropic electron–electron–core terms $f(r_{iI}, r_{jI}, r_{ij};\ \gamma)$, where $r_{ij} = r_i - r_j$, $r_{iI} = r_i - r_I$, r_i is the position of electron i, and r_I is the position of the core I. The electron–electron and the electron–core–electron terms satisfy the Kato cusp condition at $r_{ij} = 0$, and for the electron–core term, the electron–core cusp condition is enforced. The parameters α, β, and γ represent the variational parameters optimized for each Al_nC cluster using the variance minimization method.[22,23]

Diffusion Monte Carlo (DMC) simulations are then performed to remove most of the remaining variational bias to obtain the total ground-state energy. In this method, the optimized trial VMC wave function obtained in the first stage is used as a guide wave function for the importance sampling,[24,25] and an operator e^{-tH} with $t = i\tau$ is repeatedly used within the short-time approximation to propagate the trial wave function, ψ_T, in imaginary time at the long time limit to project out the system ground state or equivalently ψ_0. We have used the fixed-node approximation, which assumes that the DMC solution (ψ_0) has the same nodes of the trial wave function. For all-electron calculations, the fixed-node error is the only uncontrollable source of error in DMC, while calculations using pseudopotentials can also suffer from errors due to the nonlocality characteristic of angular momentum-dependent pseudopotentials.[26] To enforce the locality approximation due to the pseudopotentials in the calculations, we use the Casula's t-move variational scheme.[27] The core polarization correction is added to the pseudopotential to account for the core–electron correlation.[28] We used a DMC time step of 0.001 a.u. and an ensemble of 10 000 walkers. For small time steps, the bias of the DMC time step is linear to the time step, while the bias of the number of walkers is inversely proportional to the population of walkers.[29] Therefore, linear extrapolation of our DMC energies to the zero time step simultaneously removes the time step and walker population biases (when the population of walkers is assumed to be inversely proportional to the time step), as in Refs. 29 and 30. Note that we used ten times the required number of population walkers compared to the time step used. Checking the effect of the time step size with a DMC time step of 0.0005 a.u. showed that the energies within the statistical error bars remained unchanged. Such a time step leads to calculations with a high acceptance rate, e.g., greater than 99.99%. For the averages, we consider about 80 000 QMC moves.

For the Hartree–Fock (HF) calculations, we use the cc-pVQZ, cc-pV5Z, and cc-pV6Z basis sets to extrapolate to the limit of the infinitely large complete basis set (CBS). We use the two-point scheme proposed by Halkier *et al.*,[31] whose extrapolated total energy is given by $E_{CBS} = \frac{E(n_1)n_1^3 - E(n_2)n_2^3}{n_1^3 - n_2^3}$, where n_1 and n_2 are the cardinal numbers of the basis set. Most of the extrapolated values are obtained using the cc-pV5Z and cc-pV6Z basis sets; the only exception is $Al_{12}C$, where we use cc-pVQZ and cc-pV5Z.

III. RESULTS AND DISCUSSION

To determine the atomic geometric structure of the aluminum–carbon clusters, we combine first-principles molecular dynamics simulations (MD) based on DFT, as implemented in Vienna *Ab initio* Simulation Package (VASP)[32,33] to select the clusters that appear most likely in the experiments. In general, the choice of a DFT functional for the construction of the trial wavefunction in quantum Monte Carlo (QMC) calculations should be guided by its ability to accurately capture the relevant physics of the system. In Refs. 34–36, several properties of the Al_3C, Al_4C, and Al_6C clusters that are very sensitive to the exchange and correlation functionals used in the DFT calculations were investigated. The calculations have shown that the hybrid functionals provide good estimates for several properties compared to high-level calculations and experimental measurements, as also suggested by the DFT functional analysis for covalent and metallic clusters in Ref. 37. Given these data, the three-parameter exchange functional of Becke (B3) with the correlation functional of Lee, Yang, and Parr (LYP) seems to be a reasonable choice for the functionals used in this work. In addition, we performed calculations for the dimer (AlC) to obtain accurate bond lengths and binding energy values with

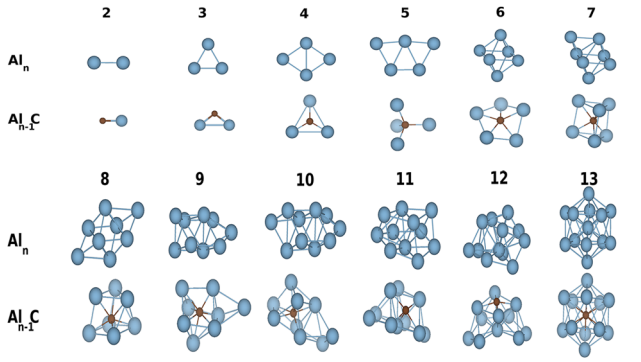

FIG. 1. The lowest energy structures of neutral Al_n and $Al_{n-1}C$ clusters (n = 2–13) determined with DFT/B3LYP using the Gaussian03 program.[17]

the experiments to ensure that the choice of the DFT functional provided a reasonable atomic structure and orbital for the trial wavefunction for the aluminum–carbon clusters. It was found that the B3LYP functional was slightly better than PBE for the bond length of the dimer (AlC) compared to the experiment. Then, within the B3LYP framework as implemented in the Gaussian program,[17] a structural reoptimization of the selected isomers is performed for consistency checking. Figure 1 shows the set of low-lying energy structures of Al_n and $Al_{n-1}C$ clusters ($n = 2, \ldots, 13$). The ground-state spin multiplicity (M_s) of Al_nC clusters is a singlet or a doublet in most cases, except for AlC and Al_2C, which are quartets and triplets, respectively. The available experimental result for the equilibrium bond length of the AlC cluster is 1.955 Å.[38] Our calculation gives a value of 1.98 Å with a difference of 0.025 Å from the experimental one. There are no experimental results available for the bond lengths of the larger clusters. Nevertheless, our values agree well with those of other theoretical approaches.[10–12]

The atomic structures of the lowest energy carbon-doped aluminum clusters were analyzed in terms of average bond length (d_{av}) and effective coordination number (η), which is defined differently from the conventional coordination number (CN) by assigning a different weight to the bonds based on their length.[39,40] Bond lengths shorter than d_{av} contribute with a weight greater than one, so η does not require a cutoff of the bond length. For structures with high symmetry, η has the same value as CN. Therefore, η is more useful in analyzing possible structural trends and has been used with great success to study the structure of various clusters,[41,42] in particular for metallic clusters.[43,44]

To better understand the influence of carbon atoms on the cluster structures, we plot in Figs. 2(a) and 2(b) the d_{av} and η, respectively, as a function of the cluster size. It is seen in Fig. 2(a) that doping one carbon atom into the aluminum clusters reduces the average bond length in comparison with the corresponding pure aluminum clusters.[43] The average bond length d_{av} reduces by more than 26% for $n \leq 5$ due to the presence of the doped carbon atom in the clusters. However, such an effect decreases almost monotonically with increasing cluster size. Notice that the average bond length d_{av} of the $Al_{12}C$ cluster approaches rapidly to that of the Al_{13} because the substitution of the central aluminum atom by a carbon atom does not cause substantial structural changes. Yet it is an icosahedral

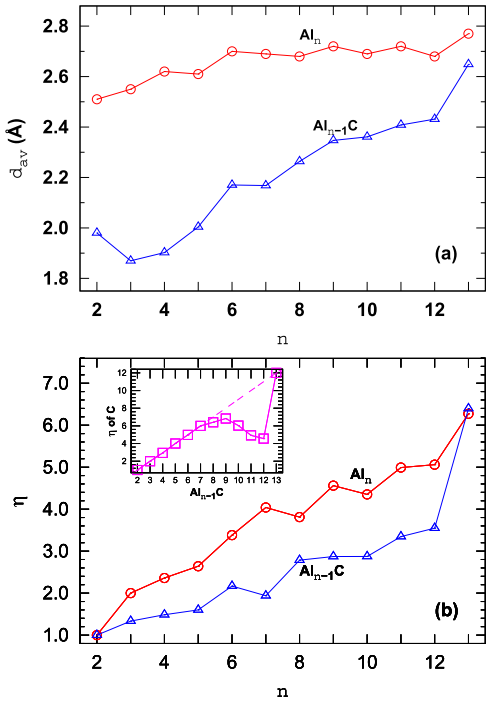

FIG. 2. (a) The weighted average bond length and (b) the effective coordination number of the $Al_{n-1}C$ and Al_n clusters as a function of cluster size n. The inset in (b) shows the effective coordination number of the carbon atom in $Al_{n-1}C$. The solid and dashed lines are a guide to the eye.

structure, as shown in Fig. 1. Figure 2(b) shows that η is sensitive enough to pick up the atomic structure changes due to substituting one aluminum atom with a carbon in the clusters. The general trend for the doped clusters follows the pure ones whose η increases almost linearly with increasing cluster size. The η of the undoped aluminum cluster shows that the aluminum neighbors increase in an even–odd alternation pattern for cluster size $n \geq 6$. The substitution of an aluminum atom by a carbon atom reduces η except for clusters with 2 and 13 atoms. It means that, for these two clusters, substituting an aluminum atom with a carbon atom should not provoke a structural change, corroborating the discussion in Fig. 2(a). The inset in Fig. 2(b) shows η of the carbon atom as a function of the cluster size. For clusters with n = 2–7 and 13, it increases linearly, as indicated by the dashed line. In these clusters, the carbon atom is equidistant to the aluminum ones; in particular, the $Al_{12}C$ cluster differs considerably from the others, forming a perfect cage for the carbon atom.

Having analyzed the atomic structure, we now proceed to the electronic structure to evaluate the electron population around the core ions as a function of cluster size using the well-known polyhedral Voronoi scheme implemented in the code CASINO.[21] Figure 3 shows the valence electron population around the C and Al ions in the $Al_{n-1}C$ clusters as a function of cluster size. The horizontal dashed lines in the figure for comparison indicate the valence electron number of a single Al and C atom. It can be seen that the substitution of an aluminum atom by carbon leads to a reduction

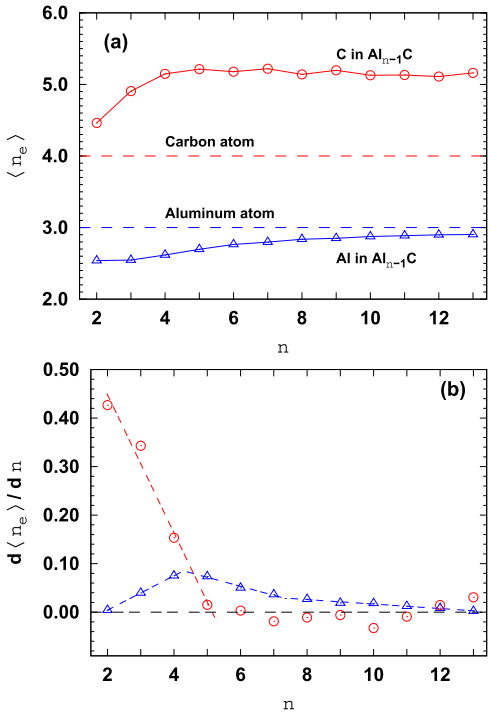

FIG. 3. (a) The average electron population and (b) the derivative of the average electron population in the $Al_{n-1}C$ cluster as a function of the cluster size n. The red circles and blue triangles are the electron populations for carbon and aluminum atoms, respectively.

in the average electron population around the aluminum ions and an increase in that around carbon, as expected by the concept of electronegativity. Note that in the dimer, the aluminum atom experiences a loss, while the carbon atom experiences a gain of about 0.5 electron charge. However, as the cluster size increases, the average electron population of the aluminum atoms in the $Al_{n-1}C$ clusters increases slowly and tends to be slightly smaller than that of the single aluminum atom. In contrast, the electron population around the carbon increases more rapidly but tends to be constant for larger clusters, with about five valence electrons. Figure 3(b) shows the derivative of the average electron population around the atoms in the clusters. The red circles and blue triangles can be interpreted as the rates of electron acceptance and donation by the carbon and aluminum atoms in the clusters, respectively. It can be seen that as the number of atoms in the clusters increases, the electron acceptance rate decreases for carbon, while it increases for aluminum up to clusters with four atoms. For larger clusters, the electron acceptance rate reaches almost zero, indicating a saturated valence electron number for carbon. In contrast, the electron donation of aluminum atoms decreases at different rates for n = 5–7 and for n = 8–13. This indicates that the nature of bonding has changed from n = 7–8, which is related to the general order of increase in the strength of interactions.

Although the correlation energy is a tiny fraction of the total energy, it has a significant effect on the atomic and electronic structure of the clusters, as shown earlier.[47–49] Table I shows the total

TABLE I. Total correlation energy E_c of the valence electrons in the Al_n and $Al_{n-1}C$ (n = 2–13) clusters. The spin multiplicity M_s of the clusters and the correlation energy difference ΔE_c between the pure and doped ones are also given. All energies are in eV units.

	Al_n		$Al_{n-1}C$		
Cluster size, n	M_s	E_c	M_s	E_c	ΔE_c
2	3	−4.882(5)	4	−4.479(8)	0.40(2)
3	2	−8.28(1)	3	−8.765(8)	−0.49(2)
4	3	−11.52(1)	2	−11.46(1)	0.06(2)
5	2	−14.58(3)	1	−14.75(2)	−0.17(3)
6	1	−18.76(2)	2	−18.26(2)	0.50(3)
7	2	−21.87(3)	1	−22.10(2)	−0.23(3)
8	1	−25.45(2)	2	−25.77(2)	−0.32(3)
9	2	−28.37(2)	1	−28.97(2)	−0.60(3)
10	1	−31.79(3)	2	−31.95(2)	−0.16(3)
11	2	−35.30(5)	1	−36.77(2)	−1.47(6)
12	1	−38.78(2)	2	−39.49(2)	−0.71(3)
13	2	−43.77(5)	1	−43.63(1)	0.14(6)

correlation energy of valence electrons E_c of the Al_n and $Al_{n-1}C$ clusters. The electron correlation energy E_c is defined as the difference between the exact ground-state energy (considered as FN-DMC energy) and the HF energy in a complete basis set limit. For the clusters under investigation, the electron correlation lowers the total ground-state energy by about 5% within the present calculations. Let us first consider the trend of correlation energy of the pure aluminum clusters Al_n with increasing cluster size. From the table, we can see that the correlation energy (E_c) increases with increasing cluster size. This is mostly due to the increase in the valence electrons, which leads to a greater screening of the Coulomb interaction between the electrons and a stronger correlation energy. Considering the doping effects of a carbon atom in the $Al_{n-1}C$ clusters, we see that, in most clusters the presence of a carbon atom leads to an increase in the correlation energy in comparison with the corresponding pure aluminum one of the same size, especially for n = 9, 11, and 12, as shown in the last column in Table I for the correlation-energy difference between the doped and undoped clusters. However, carbon doping also leads to a decrease in the correlation energy in some other clusters, such as for n = 2 and 6. This indicates that the effect of carbon doping depends strongly on the specific size and structure of the aluminum cluster, as shown in Fig. 1. In addition, doping a C atom into aluminum clusters generally leads to an increase in the spin multiplicity compared to a pure Al cluster of the same size. This is most pronounced for small clusters (e.g., n = 2 and 3). If the pure (doped) cluster has a low-spin (high-spin) configuration, the doped (pure) cluster has a high-spin (low-spin) configuration because the doped C atom offers one more valence electron to the cluster, leading to changes in the electronic and magnetic properties of the cluster. The above-mentioned calculation results demonstrate that the doping effects on the electronic structure and correlation energy of a cluster are complex and depend on several factors, including the size and structure of the cluster, and the position of the dopant. In some cases, the dopant atom can cause local distortions in the electronic structure of the cluster, leading to an increase in the correlation energy. Overall, the effect of doping

on the correlation energy of a cluster is a subtle balance between the positive and negative contributions and requires careful analysis to understand the underlying physics.

Now, we discuss the effects of the carbon atom on the atomic binding energy of the $Al_{n-1}C$ clusters. We define the binding energy per atom (BE) of the $Al_{n-1}C$ cluster as[50]

$$E_b = [E(Al_{n-1}C) - (n-1)E_a(Al) - E_a(C)]/n, \quad (2)$$

where $E(Al_{n-1}C)$, $E_a(Al)$, and $E_a(C)$ are the total energies of the cluster and the aluminum and carbon atoms, respectively, and n is the total number of atoms in the cluster.

The binding energies (E_b) of the carbon-doped aluminum clusters $Al_{n-1}C$ for $n = 2$–13 are shown in Table II. For comparison, the results of undoped aluminum clusters are also given, which are the improved results from Ref. 43. For pure aluminum clusters, E_b increases with increasing cluster size, which is consistent with previous results for other metal clusters.[44] This is also the case for the doped clusters but in the presence of alternation. The binding energies of the pure aluminum clusters obtained from our FN-DMC calculations are very close to the experimental values[46] with differences less than 5%. Moreover, a comparison with available coupled-cluster singles, doubles, and triples [CCSD(T)][36,45] values also shows good agreement. The discrepancies between the FN-DMC and CCSD(T) results could be attributed to the fixed node error in FN-DMC or a basis set error and even to the lack of higher excitations in CCSD(T). According to the FN-DMC results, substitution of an Al atom by a carbon atom in the Al_n cluster enhances the binding energy E_b of the doped $Al_{n-1}C$ cluster. The difference between the binding energies of the $Al_{n-1}C$ and Al_n clusters quantifies the gain of the binding energy due to such a substitution. In Table II, we show $\Delta E_b = E_b(Al_{n-1}C) - E_b(Al_n)$ obtained from the FN-DMC and HF calculations, denoted as ΔE_b^{FN-DMC} and ΔE_b^{HF}, respectively. The value of ΔE_b^{FN-DMC} varies between −0.295 eV (for $Al_{12}C$) and −1.022 eV (for Al_3C) as shown in Table II, accounting for 11%–41%, respectively, of the total E_b value of the clusters. In the absence of electron correlation, ΔE_b^{HF} in Table II takes into account electrostatic and exchange interactions as well as orbital relaxation (or the charge redistribution effects). The difference between ΔE_b^{FN-DMC} and ΔE_b^{HF} is the correlation contribution to ΔE_b of the clusters, denoted as ΔE_b^c. We can observe that the binding energy gain in the carbon-doped cluster is primarily due to the HF contribution of the electrostatic and exchange interactions, while the correlation contribution accounts for only a small fraction. Moreover, the doping-induced correlation gain is positive for most clusters, except for Al_2C, Al_8C, $Al_{10}C$, and $Al_{11}C$, where correlation enhances cluster stability.

In Table III, we list the dissociation energies required to decompose an Al_nC cluster through two distinct channels: $Al_{n-1}C \rightarrow Al_{n-1}$ + C and $Al_{n-1}C \rightarrow Al_{n-2}C$ + Al, defined as

$$\Delta^{(1)} = E(Al_{n-1}) + E_a(C) - E(Al_{n-1}C) \quad (3)$$

and

$$\Delta^{(2)} = E(Al_{n-2}C) + E_a(Al) - E(Al_{n-1}C), \quad (4)$$

where E is the total ground-state energy of the clusters and E_a is the ground-state energy of the atom. The FN-DMC dissociation energies for two different dissociation channels show that the energy $\Delta^{(1)}$ required to remove the C atom ranges from 2.85(1) to 7.71(3) eV, while the energy $\Delta^{(2)}$ required to remove an aluminum atom varies from 1.75(2) to 3.94(2) eV. For the same cluster size ($n \geq 3$), it is much easier to remove an aluminum atom than to remove the doped carbon atom. We also give in Table III the HF (Δ_{HF}) and electron-correlation contribution (Δ_c) to the dissociation energy of the $Al_{n-1}C$ cluster. This can help assess the extent to which electron correlation affects the stability and reactivity of the clusters, as observed in previous studies.[48–51] In particular, by

TABLE II. Binding energy per atom of the pure (Al_n) and carbon-doped aluminum ($Al_{n-1}C$) clusters. The binding energy gain (ΔE_b^{FN-DMC}) and its HF (ΔE_b^{HF}) and correlation contribution (ΔE_b^c) are also shown. Available CCSD(T) and experimental values are given for comparison. Statistical errors in FN-DMC are given in parentheses. All energies are in eV units.

	Al_n				$Al_{n-1}C$			Gain in E_b		
Cluster size, n	HF	FN-DMC	CCSD(T)[45]	Expt.[46]	HF	FN-DMC	CCSD(T)[34–36]	ΔE_b^{FN-DMC}	ΔE_b^{HF}	ΔE_b^c
2	−0.226	−0.713(6)	−0.828	−0.75	−1.307	−1.427(6)	⋯	−0.714(9)	−1.081	+0.367(9)
3	−0.521	−1.326(7)	−1.392	−1.30	−1.342	−2.200(5)	⋯	−0.874(9)	−0.821	−0.053(9)
4	−0.557	−1.482(6)	−1.606	−1.55	−1.677	−2.504(5)	−2.86	−1.022(8)	−1.120	+0.098(8)
5	−0.732	−1.695(8)	−1.795	−1.76	−1.763	−2.693(6)	−2.91	−0.998(10)	−1.031	+0.033(10)
6	−0.759	−1.932(7)	−2.066	−1.94	−1.502	−2.536(5)	⋯	−0.604(9)	−0.743	+0.139(9)
7	−0.987	−2.157(7)	−2.168	−2.12	−1.418	−2.574(5)	−2.20	−0.417(9)	−0.431	+0.014(9)
8	−0.954	−2.181(6)	⋯	−2.21	−1.435	−2.661(6)	⋯	−0.480(8)	−0.481	+0.001(8)
9	−1.017	−2.216(6)	⋯	−2.22	−1.447	−2.676(6)	⋯	−0.460(8)	−0.430	−0.030(8)
10	−1.047	−2.272(6)	⋯	−2.28	−1.412	−2.621(5)	⋯	−0.349(8)	−0.365	+0.016(8)
11	−1.081	−2.337(7)	⋯	−2.33	−1.352	−2.711(5)	⋯	−0.374(9)	−0.271	−0.103(9)
12	−1.131	−2.409(6)	⋯	−2.38	−1.414	−2.723(5)	⋯	−0.314(8)	−0.283	−0.031(8)
13	−1.110	−2.522(7)	⋯	−2.49	−1.440	−2.817(5)	⋯	−0.295(9)	−0.330	+0.035(9)

TABLE III. Dissociation energies $\Delta^{(1)}$ and $\Delta^{(2)}$ of the $Al_{n-1}C$ cluster for two different channels defined by Eqs. (3) and (4), respectively. Also given are the HF and correlation contributions to the dissociation energies. The DFT results in the literature are shown for comparison.[11] Statistical errors from the FN-DMC calculations are given in parentheses. All energies are in eV units.

Cluster size, n	FN-DMC dissociation energies						DFT[11]
	$\Delta^{(1)}$	$\Delta^{(1)}_{HF}$	$\Delta^{(1)}_{c}$	$\Delta^{(2)}$	$\Delta^{(2)}_{HF}$	$\Delta^{(2)}_{c}$	$\Delta^{(1)}$
2	2.85(1)	2.61	0.24(1)	2.85(1)	2.61	0.24(1)	···
3	5.17(1)	3.58	1.59(1)	3.74(1)	1.41	2.33(1)	6.78
4	6.04(2)	5.15	0.89(2)	3.42(1)	2.68	0.74(1)	7.32
5	7.53(2)	6.59	0.94(2)	3.45(2)	2.11	1.34(2)	6.88
6	6.74(3)	5.35	1.39(3)	1.75(2)	0.19	1.56(2)	···
7	6.42(3)	5.37	1.05(3)	2.80(2)	0.91	1.89(2)	···
8	6.19(4)	4.57	1.62(4)	3.27(3)	1.56	1.71(3)	···
9	6.63(4)	5.40	1.23(4)	2.79(3)	1.55	1.24(3)	···
10	6.27(3)	4.97	1.30(3)	2.13(3)	1.10	1.03(3)	···
11	7.10(3)	4.41	2.69(3)	3.61(3)	0.75	2.86(3)	6.07
12	6.97(6)	5.07	1.90(6)	2.86(2)	2.09	0.77(2)	7.40
13	7.71(3)	5.15	2.56(3)	3.94(2)	1.76	2.18(2)	5.84

comparing the obtained HF dissociation energies and the corresponding electron-correlation contributions, we may observe that the chemical bonding between the doped C atom and the host Al atoms in the $Al_{n-1}C$ cluster is predominantly determined by the HF interactions of the nuclei and electrons, while the electron correlation relatively plays a more important role in the bonding of an Al atom with the rest ones in the cluster.

When we compare the dissociation energies of the carbon-doped aluminum clusters with those of the undoped ones, some interesting features appear. Figure 4 shows the difference in the dissociation energies to remove an Al atom from the carbon-doped aluminum cluster $Al_{n-1}C$ and from the undoped pure aluminum cluster Al_n of the same size. The dissociation energy required to remove an Al atom from the $Al_{n-1}C$ cluster is given by $\Delta^{(2)}$, and that for the Al_n cluster is defined as $\Delta_{Al_n} = E(Al_{n-1}) + E_a(Al) - E(Al_n)$. It is seen that the difference $\Delta^{(2)} - \Delta_{Al_n}$ oscillates between positive and negative values as a function of cluster size n for $n \geq 5$. For larger

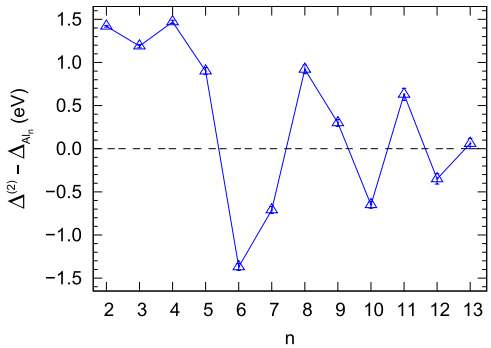

FIG. 4. The energy difference for the dissociation of an Al atom from the Al_n and $Al_{n-1}C$ clusters as a function of cluster size n.

cluster sizes, such a difference tends to zero, as expected. However, for small n, substitution of an Al atom by the doped C atom significantly affects the dissociation energy required to remove an Al atom from the systems. From such a point of view, the carbon doping enhances significantly the dissociation energy $\Delta^{(2)}$ for n = 2–5, 8, and 11 with positive values of $\Delta^{(2)} - \Delta_{Al_n}$ being larger than 0.6 eV. However, on the opposite, the carbon doping can also significantly reduce the dissociation energy for n = 6, 7, and 10 with negative values of $\Delta^{(2)} - \Delta_{Al_n}$ of a modulus larger than 0.6 eV. For n = 6, the obtained result calls attention with $\Delta^{(2)} - \Delta_{Al_n} = -1.37(4)$ eV. This indicates that the doping strongly affects the atomic structure of the cluster (as shown in Fig. 1) and it is much easier to remove an Al atom from a doped cluster at n = 6.

IV. CONCLUSIONS

In this study, we have used QMC, DFT, and HF calculations to investigate the structural and electronic properties of carbon-doped aluminum clusters. We obtained the lowest energy structures using DFT, which also provided the single-particle orbitals for the VMC trial wavefunction. Based on the optimized VMC trial wavefunction, we performed FN-DMC calculations to investigate the influence of carbon doping on the atomic and electronic structure of aluminum clusters. Our analysis showed that the obtained electron distributions and bond lengths are in agreement with the available experimental and theoretical results.

We calculated the ground-state energies of the carbon-doped clusters and estimated their atomic binding energies and dissociation energies. We found that the atomic binding energy gain due to doping is mainly from the HF contribution, while electron correlation accounts for only a small fraction of the binding energy gain. For AlC clusters, the HF contribution accounts for 151% of the total binding energy gain, while for larger clusters, such as $Al_{10}C$, it decreases to 72%.

Our study showed that the dissociation energy required to remove the carbon atom from the carbon-doped aluminum clusters ranges from 2.85(1) to 7.71(3) eV, while the dissociation energy to remove an aluminum atom varies from 1.75(2) to 3.94(2) eV. Much less energy is needed to remove an aluminum atom than to remove the carbon in these doped clusters. We also found agreement in comparing the values of the dissociation energy obtained from FN-DMC calculations to available theoretical results using different approaches in the literature. Overall, our study provides valuable insight into the properties of carbon-doped aluminum clusters that could be useful for developing new materials with desirable properties.

ACKNOWLEDGMENTS

This research was supported by CNPq, FAPEMIG, and FAPEG (Brazil). The authors acknowledge computational resources from the National Laboratory for Scientific Computing (LNCC/MCTI, Brazil) for providing HPC resources of the SDumont supercomputer (http://sdumont.lncc.br). The authors extend their sincere thanks to Dr. Juarez L. F. Da Silva and Dr. Nilton L. Moreira for their valuable contributions to this research.

AUTHOR DECLARATIONS

Conflict of Interest

The authors have no conflicts to disclose.

Author Contributions

B. G. A. Brito: Conceptualization (equal); Data curation (equal); Formal analysis (equal); Funding acquisition (supporting); Investigation (supporting); Methodology (equal); Project administration (supporting); Resources (supporting); Software (equal); Supervision (supporting); Validation (equal); Visualization (equal); Writing – original draft (equal); Writing – review & editing (equal). **G.-Q. Hai**: Conceptualization (equal); Data curation (equal); Formal analysis (equal); Funding acquisition (supporting); Investigation (supporting); Methodology (equal); Project administration (supporting); Resources (supporting); Software (equal); Supervision (supporting); Validation (equal); Visualization (equal); Writing – original draft (equal); Writing – review & editing (equal). **L. Cândido**: Conceptualization (equal); Data curation (equal); Formal analysis (equal); Funding acquisition (lead); Investigation (lead); Methodology (equal); Project administration (lead); Resources (lead); Software (equal); Supervision (lead); Validation (equal); Visualization (equal); Writing – original draft (equal); Writing – review & editing (equal).

DATA AVAILABILITY

The data that support the findings of this study are available from the corresponding author upon reasonable request.

REFERENCES

[1] P. Jena and S. N. Khanna, Mater. Sci. Eng.: A **217**, 218 (1996).
[2] S. N. Khanna and P. Jena, Phys. Rev. Lett. **69**, 1664 (1992).
[3] W.-M. Sun, Y. Li, D. Wu, and Z.-R. Li, Phys. Chem. Chem. Phys. **14**, 16467 (2012).
[4] D. E. Bergeron, P. J. Roach, A. W. Castleman, Jr., N. O. Jones, and S. N. Khanna, Science **307**, 231 (2005).
[5] R. B. King and J. Zhao, Chem. Commun. **2006**, 4204.
[6] J. Zhao, B. Liu, H. Zhai, R. Zhou, G. Ni, and Z. Xu, Solid State Commun. **122**, 543 (2002).
[7] B. D. Leskiw and A. W. Castleman, Jr., Chem. Phys. Lett. **316**, 31 (2000).
[8] X. Li and L.-S. Wang, Phys. Rev. B **65**, 153404 (2002).
[9] Q. Luo, Phys. Chem. Chem. Phys. **14**, 14878 (2012).
[10] C. Ashman, S. N. Khanna, and M. R. Pederson, Chem. Phys. Lett. **324**, 137 (2000).
[11] B. K. Rao and P. Jena, J. Chem. Phys. **115**, 778 (2001).
[12] S. F. Li and X. G. Gong, Phys. Rev. B **70**, 075404 (2004).
[13] P. Hohenberg and W. Kohn, Phys. Rev. **136**, B864 (1964).
[14] W. Kohn and L. J. Sham, Phys. Rev. **140**, A1133 (1965).
[15] A. D. Becke, J. Chem. Phys. **98**, 5648 (1993).
[16] C. Lee, W. Yang, and R. G. Parr, Phys. Rev. B **37**, 785 (1988).
[17] M. J. Frisch, G. W. Trucks, H. B. Schlegel, G. E. Scuseria, M. A. Robb, J. R. Cheeseman, J. A. Montgomery, Jr., T. Vreven, K. N. Kudin, J. C. Burant, J. M. Millam, S. S. Iyengar, J. Tomasi, V. Barone, B. Mennucci, M. Cossi, G. Scalmani, N. Rega, G. A. Petersson, H. Nakatsuji, M. Hada, M. Ehara, K. Toyota, R. Fukuda, J. Hasegawa, M. Ishida, T. Nakajima, Y. Honda, O. Kitao, H. Nakai, M. Klene, X. Li, J. E. Knox, H. P. Hratchian, J. B. Cross, V. Bakken, C. Adamo, J. Jaramillo, R. Gomperts, R. E. Stratmann, O. Yazyev, A. J. Austin, R. Cammi, C. Pomelli, J. W. Ochterski, P. Y. Ayala, K. Morokuma, G. A. Voth, P. Salvador, J. J. Dannenberg, V. G. Zakrzewski, S. Dapprich, A. D. Daniels, M. C. Strain, O. Farkas, D. K. Malick, A. D. Rabuck, K. Raghavachari, J. B. Foresman, J. V. Ortiz, Q. Cui, A. G. Baboul, S. Clifford, J. Cioslowski, B. B. Stefanov, G. Liu, A. Liashenko, P. Piskorz, I. Komaromi, R. L. Martin, D. J. Fox, T. Keith, M. A. Al-Laham, C. Y. Peng, A. Nanayakkara, M. Challacombe, P. M. W. Gill, B. Johnson, W. Chen, M. W. Wong, C. Gonzalez, and J. A. Pople, GAUSSIAN 03, Revision C.02, Gaussian, Inc., Wallingford, CT, 2004.
[18] B. P. Pritchard, D. Altarawy, B. Didier, T. D. Gibson, and T. L. Windus, J. Chem. Inf. Model. **59**, 4814 (2019).
[19] J. R. Trail and R. J. Needs, J. Chem. Phys. **122**, 014112 (2005).
[20] J. R. Trail and R. J. Needs, J. Chem. Phys. **122**, 174109 (2005).
[21] R. J. Needs, M. D. Towler, N. D. Drummond, P. López Ríos, and J. R. Trail, J. Chem. Phys. **152**, 154106 (2020).
[22] P. R. C. Kent, R. J. Needs, and G. Rajagopal, Phys. Rev. B **59**, 12344 (1999).
[23] N. Drummond and R. Needs, Phys. Rev. B **72**, 085124 (2005).
[24] D. M. Ceperley and B. J. Alder, J. Chem. Phys. **81**, 5833 (1984).
[25] L. Cândido, B. G. A. Brito, J. N. Teixeira Rabelo, and G.-Q. Hai, J. Cluster Sci. **32**, 813 (2021).
[26] R. Nazarov, L. Shulenburger, M. Morales, and R. Q. Hood, Phys. Rev. B **93**, 094111 (2016).
[27] M. Casula, Phys. Rev. B **74**, 161102 (2006).
[28] E. L. Shirley and R. M. Martin, Phys. Rev. B **47**, 15413 (1993).
[29] N. D. Drummond, J. R. Trail, and R. J. Needs, Phys. Rev. B **94**, 165170 (2016).
[30] C. J. Umrigar, M. P. Nightingale, and K. J. Runge, J. Chem. Phys. **99**, 2865 (1993).
[31] A. Halkier, T. Helgaker, P. Jørgensen, W. Klopper, H. Koch, J. Olsen, and A. K. Wilson, Chem. Phys. Lett. **286**, 243 (1998).
[32] G. Kresse and J. Hafner, Phys. Rev. B **48**, 13115 (1993).
[33] G. Kresse and J. Furthmüller, Phys. Rev. B **54**, 11169 (1996).
[34] A. I. Boldyrev, J. Simons, X. Li, W. Chen, and L.-S. Wang, J. Chem. Phys. **110**, 8980 (1999).
[35] D. Y. Zubarev and A. I. Boldyrev, J. Chem. Phys. **122**, 144322 (2005).
[36] H. Yang, Y. Zhang, and H. Chen, J. Chem. Phys. **141**, 064302 (2014).
[37] C. R. Hsing, C. M. Wei, N. D. Drummond, and R. J. Needs, Phys. Rev. B **79**, 245401 (2009).
[38] C. R. Brazier, J. Chem. Phys. **98**, 2790 (1993).
[39] R. Hoppe, Angew. Chem., Int. Ed. Engl. **9**, 25 (1970).
[40] R. Hoppe, Z. Kristallogr. - Cryst. Mater. **150**, 23 (1979).
[41] B. G. A. Brito, G.-Q. Hai, and L. Cândido, Phys. Rev. A **98**, 062508 (2018).
[42] E. M. Isaac Moreira, B. G. A. Brito, G.-Q. Hai, and L. Cândido, Chem. Phys. Lett. **754**, 137636 (2020).
[43] L. Cândido, J. N. Teixeira Rabelo, J. L. F. da Silva, and G.-Q. Hai, Phys. Rev. B **85**, 245404 (2012).
[44] B. G. A. Brito, G.-Q. Hai, and L. Cândido, J. Chem. Phys. **146**, 174306 (2017).
[45] V. O. Kiohara, E. F. V. Carvalho, C. W. A. Paschoal, F. B. C. Machado, and O. Roberto-Neto, Chem. Phys. Lett. **568**, 42 (2013).
[46] U. Ray, M. F. Jarrold, J. E. Bower, and J. S. Kraus, J. Chem. Phys. **91**, 2912 (1989).
[47] B. G. A. Brito, G.-Q. Hai, and L. Cândido, J. Chem. Phys. **151**, 014303 (2019).
[48] V. G. de Pina, B. G. A. Brito, G.-Q. Hai, and L. Cândido, Phys. Chem. Chem. Phys. **23**, 9832 (2021).
[49] E. M. I. Moreira, B. G. A. Brito, G.-Q. Hai, and L. Cândido, Phys. Chem. Chem. Phys. **24**, 3119 (2022).
[50] N. L. Moreira, B. G. A. Brito, J. N. T. Rabelo, and L. Cândido, J. Comput. Chem. **37**, 1531 (2016).
[51] B. G. A. Brito, G.-Q. Hai, and L. Cândido, Chem. Phys. Lett. **804**, 139888 (2022).